Human Molecular Genetics, 2004, Vol. 13, No. 12 ***1257–1265***
DOI: 10.1093/hmg/ddh139
Advance Access published on April 28, 2004

Ataxin-7 is a subunit of GCN5 histone acetyltransferase-containing complexes

Dominique Helmlinger[1], Sara Hardy[2], Souphatta Sasorith[3], Fabrice Klein[1], Flavie Robert[2], Chantal Weber[1], Laurent Miguet[4], Noëlle Potier[4], Alain Van-Dorsselaer[4], Jean-Marie Wurtz[3], Jean-Louis Mandel[1], Làszlò Tora[2] and Didier Devys[1,*]

[1]Department of Molecular Pathology, [2]Department of Transcription and [3]Department of Structural Genomics and Biology, Institut de Génétique et de Biologie Moléculaire et Cellulaire, CNRS/INSERM/ULP, BP 10142, 67404 Illkirch Cedex, France and [4]Laboratoire de Spectrométrie de Masse Bio-Organique, CNRS UMR7509, 67087 Strasbourg, France

Received February 16, 2004; Revised April 2, 2004; Accepted April 19, 2004

Spinocerebellar ataxia type 7 (SCA7) is a neurodegenerative disorder caused by a CAG repeat expansion in the *SCA7* gene leading to elongation of a polyglutamine tract in ataxin-7, a protein of unknown function. A putative ataxin-7 yeast orthologue (SGF73) has been identified recently as a new component of the SAGA (Spt/Ada/Gcn5 acetylase) multisubunit complex, a coactivator required for transcription of a subset of RNA polymerase II-dependent genes. We show here that ataxin-7 is an integral component of the mammalian SAGA-like complexes, the TATA-binding protein-free TAF-containing complex (TFTC) and the SPT3/TAF9/GCN5 acetyltransferase complex (STAGA). In agreement, immunoprecipitation of ataxin-7 retained a histone acetyltransferase activity, characteristic for TFTC-like complexes. We further identified a minimal domain in ataxin-7 that is required for interaction with TFTC/STAGA subunits and is conserved highly through evolution, allowing the identification of a *SCA7* gene family. We showed that this domain contains a conserved Cys_3His motif that binds zinc, forming a new zinc-binding domain. Finally, polyglutamine expansion in ataxin-7 did not affect its incorporation into TFTC/STAGA complexes purified from SCA7 patient cells. We demonstrate here that ataxin-7 is the human orthologue of the yeast SAGA SGF73 subunit and is a bona fide subunit of the human TFTC-like transcriptional complexes.

INTRODUCTION

Spinocerebellar ataxia type 7 (SCA7) is a dominantly inherited neurodegenerative disorder, characterized by late-onset neuronal loss in cerebellum, brainstem and retina. SCA7 is caused by a CAG repeat expansion (38–460) in the *SCA7* gene encoding ataxin-7, a 892 amino acids protein of unknown function (1,2). Initial sequence analysis only predicted a bipartite nuclear localization signal (NLS) shown to be functional in transfected cells (3). However, recent bioinformatic studies identified a significant block of homology between human ataxin-7 and a yeast open reading frame, *YGL066w* (4,5), which was identified recently as a novel subunit of the SAGA complex (Spt/Ada/Gcn5 acetylase) and named SGF73 (6,7).

The yeast SAGA complex is composed of Ada coactivators, Spt proteins, a subset of yeast TATA-binding protein (TBP)-associated factors (TAFs) and Tra1 (8,9). The yeast SAGA acts as a transcriptional coactivator/adapter required at specific promoters and possesses histone acetyltransferase (HAT) activity that is mediated by Gcn5. Human homologues of yeast Gcn5 include PCAF and GCN5 (10,11), which were found in several multiprotein complexes, such as TBP-free TAF complex (TFTC) (12), SPT3/TAF9/GCN5 acetyltransferase complex (STAGA) (13) and PCAF/GCN5 complexes (14). While still incompletely characterized, these multisubunit complexes show related, but not identical, compositions and presumably overlapping but also distinct functions. All contain TRRAP, the human homologue of yeast Tra1, homologues of yeast SAGA subunits and a subset of TAFs, but clearly lack the TBP (15). However, TFTC specifically contained TAF5 and TAF6, whose yeast homologues are also found in SAGA, whereas these subunits were not found in STAGA or in PCAF/GCN5 complexes (16). These complexes

*To whom correspondence should be addressed. Email: devys@igbmc.u-strasbg.fr

contain a GCN5 HAT activity and were shown to acetylate preferentially histone H3 in both free and nucleosomal contexts and to activate transcription on chromatin templates (12,17,18). Furthermore, TFTC was shown to direct preinitiation complex assembly in the absence of transcription factor IID (TFIID) on naked DNA templates (19). Recent findings also suggested a role for TFTC/STAGA complexes in DNA repair (17,20).

In this study, we demonstrated that ataxin-7 is an integral subunit of highly purified TFTC complex and that an anti-ataxin-7 antibody co-immunoprecipitated TFTC-like complexes and an HAT activity corresponding to that of GCN5. Furthermore, we identified a family of *SCA7* genes conserved from human to yeast. Biochemical experiments showed that a highly conserved domain in ataxin-7 was able to bind zinc and was sufficient for interaction with TFTC/STAGA subunits. Finally, we showed that a polyglutamine (polyQ) expansion in ataxin-7 did not affect TFTC-like complex formation.

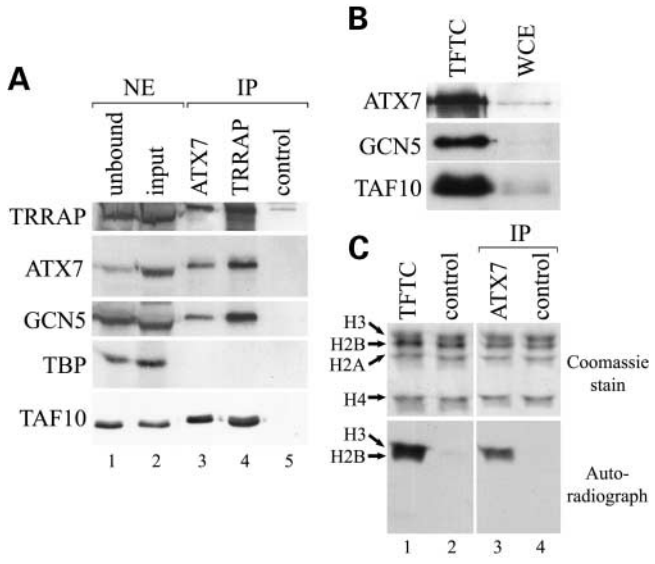

Figure 1. Ataxin-7 is an integral component of TFTC-like complexes *in vivo*. (**A**) Crude HeLa nuclear extracts (NEs) were immunoprecipitated with anti-ataxin-7, anti-TRRAP polyclonal antibodies or non-immune rabbit serum as a negative control. Part of immunoprecipitated complexes retained on protein A–sepharose beads were either tested for HAT activity (C) or analyzed by immunoblotting with monoclonal antibodies specifically detecting TFTC/STAGA subunits, as indicated. A TFIID-specific subunit, TBP, was not found in complexes immunoprecipitated with anti-ataxin-7 or TRRAP antibodies. Equal amounts of NEs before (input) and after (unbound) TRRAP IP were loaded. (**B**) Ataxin-7, GCN5 and TAF10 were present and enriched significantly in a highly purified TFTC fraction (19), when compared with HeLa crude whole cell extract (WCE). (**C**) Autoradiograph of HAT assay performed on ataxin-7 immunopurified fraction (lane 3) or control IP (lane 4) shown in (A). This assay (bottom) was performed by adding tritiated acetyl-CoA and purified histones (shown by Coomassie blue staining in the top) directly to immunopurified complexes retained on sepharose beads. Highly purified TFTC was used as a positive control (TFTC; lane 1) and omission of sepharose beads was used as a negative control (lane 2).

RESULTS

Ataxin-7 is a novel subunit of GCN5 HAT-containing complexes

A putative ataxin-7 yeast orthologue (SGF73, encoded by *YGL066w*) has been identified recently as a novel subunit of the SAGA complex (7). We thus asked whether human ataxin-7 is also a subunit of TFTC/STAGA complexes which are human homologues of the yeast SAGA complex. In order to test this hypothesis, we performed co-immunoprecipitation (IP) experiments using nuclear extract (NE) of HeLa cells. When an anti-ataxin-7 antibody was used to immunoprecipitate ataxin-7-associated proteins, we detected by western blot analysis ataxin-7 and the specific TFTC subunits TRRAP and GCN5 (Fig. 1A, lane 3), whereas these proteins were not detected in a control IP (Fig. 1A, lane 5). In addition, the anti-ataxin-7 antibody also immunoprecipitated TAF10, but not TBP. Conversely, an anti-TRRAP antibody immunopurified ataxin-7 together with other human TFTC subunits, as shown by western blotting (Fig. 1A, lane 4) and mass spectrometry (data not shown). These results suggest that ataxin-7 is associated with TRRAP in a large multiprotein complex. Importantly, an anti-TBP antibody failed to detect TBP in both ataxin-7- and TRRAP-immunopurified fractions (Fig. 1A, lanes 3 and 4), suggesting that human ataxin-7 is a component of TFTC, but not of TFIID, which specifically contains TBP. Comparison of the band intensities derived from equal quantities of crude NEs before (NE input, lane 2) or after (NE unbound, lane 1) TRRAP IP indicated that a significant amount of endogenous ataxin-7 is associated with TFTC-like complexes *in vivo* (lanes 3 and 4).

These results were further confirmed by using highly purified TFTC preparation (19). A monoclonal antibody against human ataxin-7 strongly and specifically detected a band at the expected size (110 kDa) in the highly purified TFTC complex (Fig. 1B). These results together unequivocally confirmed that ataxin-7 is a TFTC/STAGA subunit.

TFTC/STAGA complexes contain a HAT activity that is mediated by GCN5 (12). In order to confirm that endogenous ataxin-7 is an integral component of these complexes, we tested the ability of the ataxin-7 immunopurified complex to acetylate free histones using an *in vitro* assay. This assay was performed directly on sepharose beads after IP. As shown in Figure 1C, the ataxin-7 immunopurified fraction efficiently acetylated histone H3 and to a lesser extent histone H2B (lane 3). As a positive control, purified TFTC showed a similar pattern of histone acetylation (lane 1). In contrast no HAT activity was detected in control IP (lane 4). Altogether, these results demonstrated that human ataxin-7 is a novel subunit of GCN5 histone acetylase-containing complex TFTC/STAGA *in vivo* and thus likely the human orthologue of yeast SGF73 SAGA component.

Identification of conserved domains in ataxin-7

As ataxin-7 and SGF73 are part of an important evolutionarily conserved complex acting in eukaryotic transcriptional regulation, we next wanted to determine the pattern of ataxin-7 sequence conservation through evolution and searched for *SCA7* homologue genes in various genomes. Four *SCA7* paralogue genes were identified in the human genome and named *SCA7*, *SCA7-L1*, *SCA7-L2* and *SCA7-L3*, encoding ATX7, ATX7-L1, ATX7-L2 and ATX7-L3, respectively (Fig. 2).

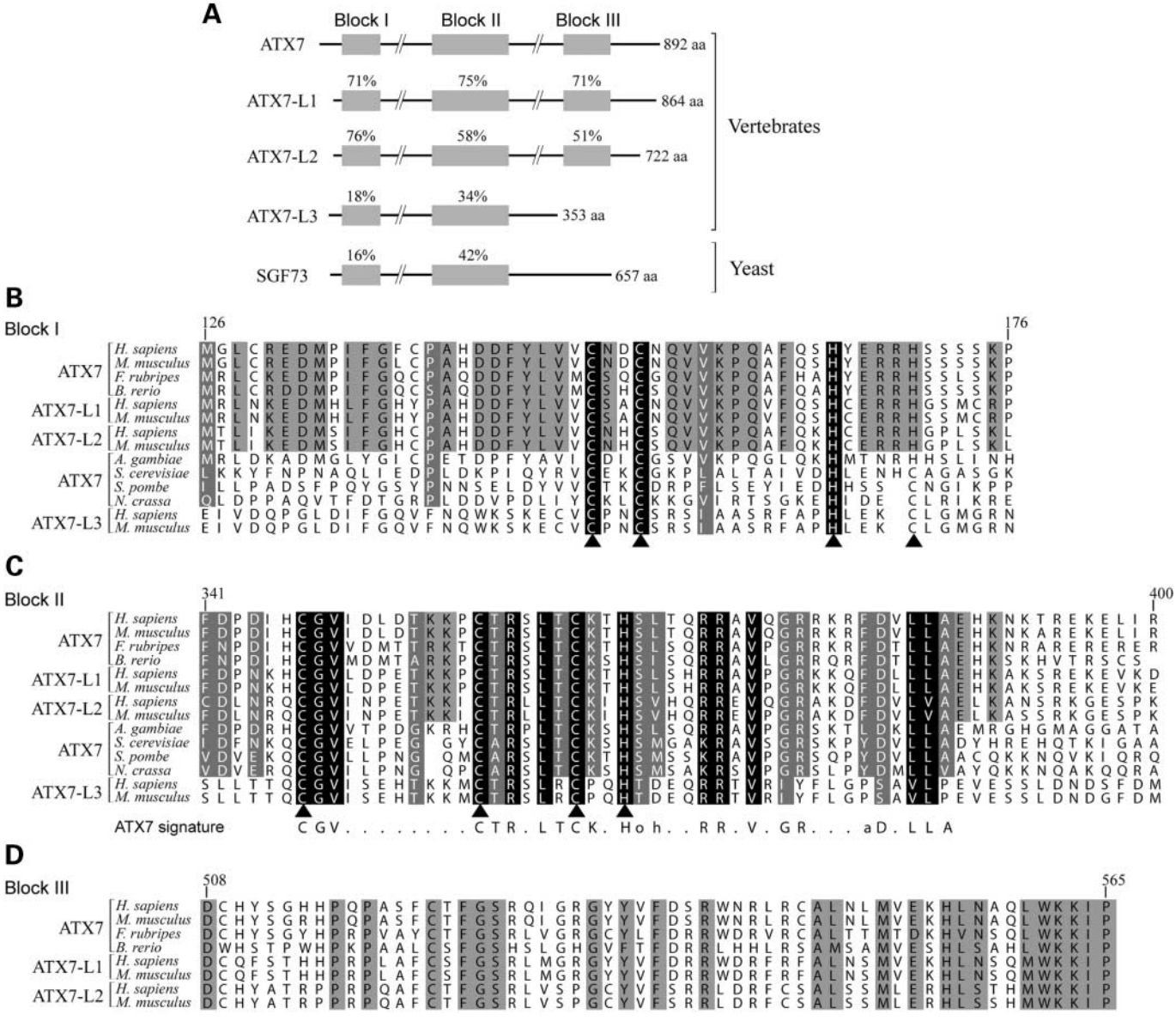

Figure 2. Identification of conserved domains in ATX7 homologues. (**A**) Schematic representation of the ATX7 family in vertebrates (human, mouse and fish) and in yeast. For each conserved block (grey boxes), sequence identities of human ATX7 paralogues and yeast SGF73 are indicated relative to human ATX7. (**B**–**D**) Sequence alignment of ATX7 conserved block I (B) (residues 126–176, according to the numbering of the human sequence), block II (C) (residues 341–400) and of block III (D) (residues 508–565). Conserved residues with >80% identity are indicated in white with black shading, conserved residues between 60% and 80% identity are shown in white with dark grey shading and residues with >80% identity within vertebrates are shown in black with light grey shading. Below the alignment, conserved His and Cys are labelled (black triangles). Block II consensus sequence is also indicated: o for alcohol residues (Ser or Thr), h for hydrophobic residues (Leu, Ile, Val or Met) and a for aromatic residues (Phe or Tyr). GenBank/SwissProt/TrEmbl accession numbers are: *Homo sapiens* ATX7 (Q9Y6P8), ATX7-L1 (Q9ULK2), ATX7-L2 (NP_699171), ATX7-L3 (Q8IY68); *Mus musculus* ATX7 (Q8BL17), -L1 (XM_354666), -L2 (Q8C8K6), -L3 (Q8C1T7); *Fugu rubripes* ATX7 (CAAB01000009), *Brachydanio rerio* ATX7 (CD594184), *Anopheles gambiae* (Q7Q561), *Saccharomyces cerevisiae* (P53165), *Schizosaccharomyces pombe* (O94397) and *Neurospora crassa* (Q7S113). All human and mouse ATX7 paralogues are shown, whereas only ATX7 orthologue is shown for each other species.

These genes are unambiguous *SCA7* paralogues as they were localized at distinct loci and found consistently in all vertebrate genomes analyzed (*Homo sapiens*, *Mus musculus*, *Brachydanio rerio* and *Fugu rubripes*). Sequence comparison of ATX7 family members revealed two conserved blocks: block I (residues 126–176 in human ATX7) and block II (residues 341–400). A third region (block III, residues 508–565) was conserved in all vertebrate sequences except in ATX7-L3 (Fig. 2A). The expandable polyQ motif is present and located N-terminal to block I in human ATX7 and in its vertebrate orthologues but is absent in ATX7 paralogues.

Using human ATX7 blocks I and II as query sequences, we retrieved several ATX7 homologues in more distant species: *Ciona intestinalis* (data not shown), *Anopheles gambiae*,

Caenorhabditis briggsae (data not shown), *Saccharomyces cerevisiae*, *Schizosaccharomyces pombe* and *Neurospora crassa.* In these genomes, a single ATX7 sequence was found and characterized by a weakly conserved block I (16% identity between *H. sapiens* and *S. cerevisiae*) located N-terminal to a highly conserved block II (42% identity) and by absence of block III (Fig. 2A). This pattern and degree of conservation suggest that these yeast proteins are ATX7 orthologues. Interestingly, ATX7-L3 was also characterized by the absence of block III and showed a weaker homology to human ATX7 (34% identity for block II) than SGF73 (42% identity for block II). This suggested that *SCA7-L3* might result from an ancient duplication of an ancestral *SCA7* gene. Multiple alignments of the highly conserved block II identified several invariant residues across species allowing the definition of an ATX7 signature, as shown in Figure 2C. In particular, block II contained 3 Cys and 1 His (Cys_3His, black triangles in Fig. 2C) forming a Cys-X_{9-10}-Cys-X_5-Cys-X_2-His motif within a specific signature that was found only in ATX7 and its homologues.

Ataxin-7 is a zinc-binding protein

As ataxin-7 block II contained invariant residues with the potential to coordinate metal ions, we next asked whether human ataxin-7 binds a metal through this highly conserved domain. We constructed an expression vector that enabled the production of an ataxin-7 fragment (residues 311–406) encompassing block II fused to glutathione *S*-transferase (GST). After removal of the GST moiety (Fig. 3A), metal content of the purified recombinant ataxin-7 fragment was analyzed by electrospray ionization-mass spectrometry (ESI-MS). Measurements were performed in ammonium acetate for native conditions and in water–acetonitrile with formic acid for denaturing conditions. Under denaturing conditions, we detected one major ionization product of 12 848.7 $\pm$ 0.3 Da, fitting with ataxin-7 fragment theoretical mass of 12 848.4 Da (data not shown). Under non-denaturing conditions, we detected one major product of 12 911.5 $\pm$ 0.2 Da, revealing the presence of one zinc atom as deduced by comparing molecular masses obtained from denaturing and native conditions (Fig. 3B). No other ionization products of higher molecular weight were detected, indicating that this domain was monomeric in these conditions. Together, these results showed that this conserved block II corresponds to a folded zinc-binding domain (ZBD), confirming the functional relevance of the highly conserved Cys and His residues. This ataxin-7 domain (residues 311–406) is thereafter referred as ataxin-7 ZBD.

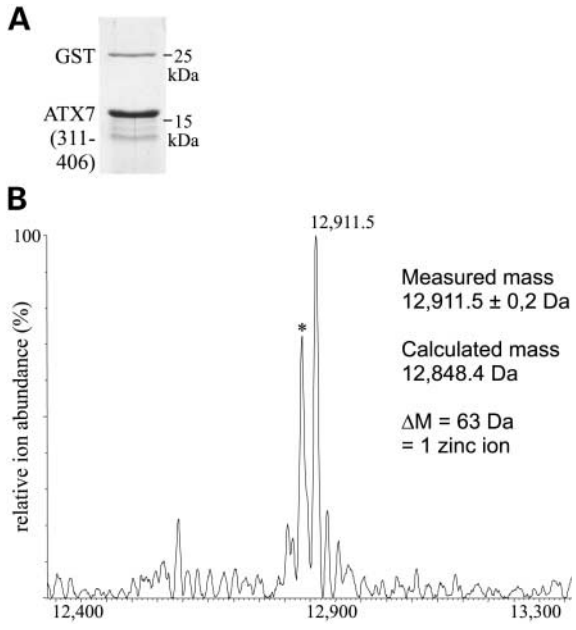

Figure 3. Mass spectrometry measurements of ataxin-7 block II (residues 311–406). (**A**) Coomassie blue-stained SDS–PAGE of ATX7 (311–406). (**B**) Real mass spectrum of ATX7 (311–406) under native conditions, in ammonium acetate. The mass difference between the measured mass and the expected mass shows the binding of one single zinc atom per molecule. The peak marked with an asterisk corresponds to species showing a loss of 28 Da and was also detected under denaturing conditions (data not shown).

Human ataxin-7 ZBD interacts with TFTC/STAGA subunits

We next wanted to examine whether the highly conserved ZBD could directly recruit TFTC/STAGA complexes. We cloned and expressed the following fusion proteins: GST–ATX7 (311–406) which corresponds to the ZBD and GST–ATX7 (90–406) encompassing the block I and the ZBD (Fig. 4A). These recombinant proteins were produced and immobilized on glutathione–sepharose beads in parallel with GST alone as a control. We then tested the ability of these fusion proteins to interact with TFTC/STAGA subunits from HeLa NE. As shown by western blot analysis (Fig. 4B), all TFTC/STAGA subunits tested, TRRAP, GCN5 and TAF10, were recruited specifically from NEs by GST–ATX7 (311–406) and by GST–ATX7 (90–406), but not by the GST control. In contrast, ataxin-7 ZBD did not interact with TIF1β, which is a factor unrelated to these complexes. Interestingly, endogenous human ataxin-7, which is expressed at low levels in HeLa cells, was enriched significantly in the GST–ATX7-bound fraction when compared with the input NE. This result further suggests that the different GST–ATX7 fusion proteins pull-down entire TFTC-like complexes of which endogenous ataxin-7 is an integral component in HeLa cells.

To further delineate the domain interacting with TFTC subunits, we performed successive deletions of the GST–ATX7 (311–406) initial construct, removing the weakly conserved residues in the ZBD N- and C-terminal ends. Using five deletion constructs (Fig. 4A), we defined a minimal ZBD (330–401) that is sufficient to pull-down GCN5 and TAF10 (Fig. 4C).

PolyQ expansion in ataxin-7 does not affect TFTC-like complexes formation

The SCA7 mutation is an expansion of a polyQ tract in ataxin-7 N-terminal part (Fig. 4A) which confers a gain of function to the mutant protein. SCA7 belongs to a group of neurodegenerative disorders, including Huntington's disease, caused

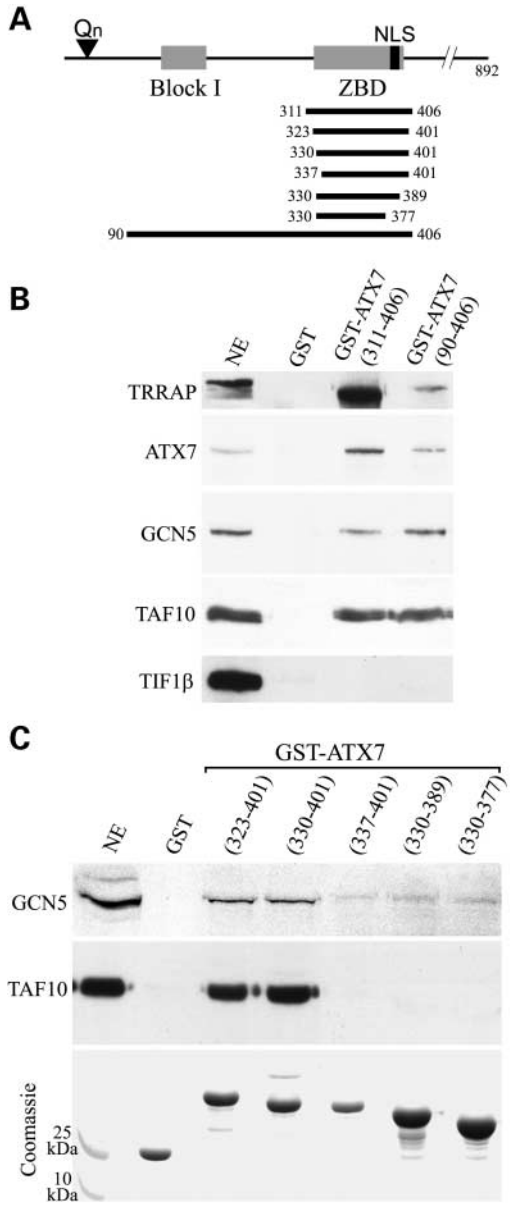

Figure 4. Ataxin-7 zinc-binding domain (ZBD) is sufficient to pull-down TFTC/STAGA complexes from HeLa nuclear extracts (NEs). (**A**) Schematic representation of human ataxin-7 domains. Grey boxes correspond to the block I and to the ZBD. The polyQ motif and the NLS are also shown. The different fusion proteins used in GST pull-down assays are represented according to their respective length. (**B**, **C**) Crude HeLa NEs were used for pull-down assays with recombinant GST or GST–ATX7 fusion proteins bound to glutathione–sepharose beads. Precipitates were analyzed by immunoblotting to detect the proteins indicated (B and top in C) or by Coomassie blue staining (bottom in C). Input NE equals 10%.

by a polyQ expansion. A hallmark of these disorders is the aggregation of polyQ proteins into insoluble nuclear inclusions (NIs).

First, we wanted to determine whether the polyQ expansion would affect the association of ataxin-7 with TFTC/STAGA complexes. We performed co-IP experiments using whole cell extracts (WCEs) of HEK293 cells transfected with constructs expressing FLAG-tagged full-length ataxin-7 carrying either 10 or 60 glutamines. Anti-FLAG immunoprecipitated fractions were analyzed by western blot analysis. Interestingly, normal and mutant ataxin-7 equally interacted with the TFTC subunits TRRAP, GCN5 and TAF10 (Fig. 5A). These proteins were not detected after anti-FLAG IP performed on mock transfected HEK293 cells (Fig. 5A). Normal and mutant recombinant ataxin-7 were immunoprecipitated specifically and efficiently using anti-FLAG antibody. In order to confirm this result *in vivo*, we performed co-IP experiments using lymphoblastoid cell lines, derived from an SCA7 patient, expressing both normal (10 Q) and mutant (51 Q) ataxin-7 (Fig. 5B, lane 1). Both normal and mutant ataxin-7 were immunoprecipitated specifically from NEs of SCA7 cells with an anti-TRRAP (Fig. 5B, lane 2) or with an anti-ataxin-7 antibody (Fig. 5B, lane 3). The bands corresponding to normal and expanded ataxin-7 were of comparable intensities in both TRRAP and ataxin-7 IPs, indicating that both forms of ataxin-7 are equally incorporated within TFTC/STAGA complexes in SCA7 cells. Two percent of the amount of NE used for IP was loaded on the gel (Fig. 5B, lane 1) and revealed that endogenous ataxin-7 was enriched significantly after TRRAP IP (Fig. 5B, lane 2). Furthermore, we performed an anti-TRRAP IP using NEs from SCA7 cells used in Figure 5B or from control lymphoblastoid cells derived from an unaffected individual, only expressing normal ataxin-7. Western blot analysis of TRRAP-associated proteins showed that GCN5 and TAF10 were similarly immunopurified from both cell lines (Fig 5C, lanes 2 and 3). Ten percent of the amount of NE used for IP was loaded on the gel (Fig. 5C, lane 1) and revealed that endogenous TRRAP was enriched efficiently after IP (Fig. 5C, lane 2), in both the control and the SCA7 cell line. These results together indicate that TFTC/STAGA subunit composition is not altered by polyQ expansion in ataxin-7.

We then investigated whether expanded ataxin-7 would recruit and sequester TFTC/STAGA subunits into NIs. We transfected truncated *SCA7* cDNA constructs with 10 or 60 CAG encompassing the block I, the ZBD and the NLS. Immunostaining revealed that normal and mutant recombinant ataxin-7 were localized exclusively in the nucleus from HeLa (Fig. 5B), COS-1, NIH-3T3 and HEK293 cells (data not shown), confirming that the predicted bipartite NLS is functional in these cells. This result is surprisingly contradictory with a recent study suggesting that this NLS was not functional by using a comparable ataxin-7 construct (residues 1–460) in transfection experiments using HEK293 cells (21). Mutant ataxin-7 (residues 1–456) either displayed a diffuse nuclear staining or accumulated into large NIs (Fig. 5B). Endogenous TAF10 showed an identical homogenous nuclear localization in HeLa cells transfected with either normal or mutant *SCA7* constructs. In particular, TAF10 was not recruited in NIs and not depleted from its normal localization (Fig. 5B). Similar results were obtained for TRRAP (data not shown). Altogether, these results show that ataxin-7 incorporation into TFTC/STAGA complexes is not altered by a polyQ expansion and that nuclear distribution of TFTC/STAGA subunits (TAF10, TRRAP) is not affected by mutant ataxin-7 aggregation in transfected cells.

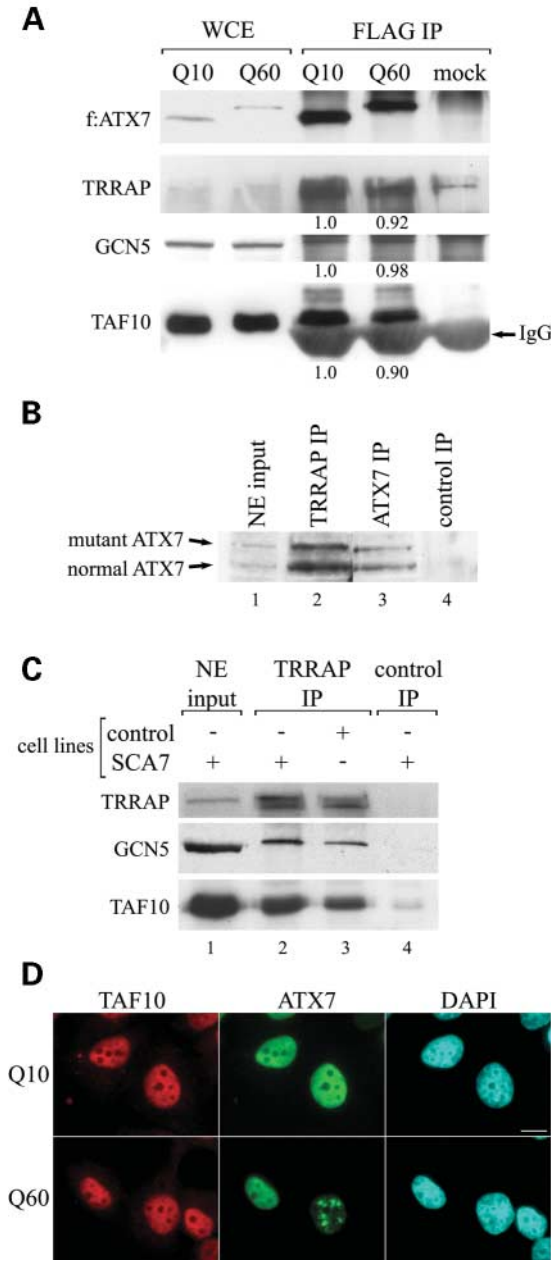

Figure 5. PolyQ expansion in ataxin-7 does not affect TFTC/STAGA complexes formation and localization. (**A**) WCEs of HEK293 cells were transfected with pc7NFL (Q10), pc7EFL (Q60) or empty vector (mock) and immunoprecipitated with anti-FLAG monoclonal antibody. Immunopurified fractions were analyzed by immunoblotting with antibodies specifically detecting TFTC/STAGA subunits, as indicated. Input HEK293 WCEs equal 2.5%. Signal intensities measured by densitometer are indicated for each subunit after normalization to immunoprecipitated recombinant ataxin-7. Ratios were calculated relative to that obtained after normal ataxin-7 (Q10) IP. These results are representative of three independent experiments. (**B**) NEs of SCA7 lymphoblastoid cells were immunoprecipitated with anti-ataxin-7, anti-TRRAP polyclonal antibodies or non-immune rabbit serum as a negative control. Input SCA7 lymphoblastoid NEs equals 2% (lane 1). (**C**) NEs of control and SCA7 lymphoblastoid cells were immunoprecipitated with anti-TRRAP polyclonal antibody. NEs of SCA7 cells were immunoprecipitated with non-immune rabbit serum as a negative control (control IP, lane 4). Immunopurified fractions were analyzed by immunoblotting with antibodies specifically detecting TFTC/STAGA subunits, as indicated. Input SCA7 lymphoblastoid NEs equals 10% (lane 1). (**D**) Immunolocalization of endogenous TAF10 (red) and transiently expressed ataxin-7 (residues 1–456) (green) carrying 10 Qs (top) or 60 Qs (bottom). Pseudocoloured images of nuclei counterstained with DAPI revealed exclusive nuclear localization of both proteins. Scale bar represents 10 μm.

DISCUSSION

Identification and multiple alignments of ATX7 homologues revealed significant conservation of three blocks. Block II is conserved highly through evolution, from human to yeast, and allowed us to define an ATX7 signature (Fig. 2C). Notably, we noticed strictly conserved Cys and His forming a Cys-X_{9-10}-Cys-X_5-Cys-X_2-His motif that exhibits similarities with the Nup475 family consensus sequence (Cys-X_8-Cys-X_5-Cys-X_3-His). This domain has been shown previously to coordinate zinc through the conserved Cys and His residues and to fold into a new structural zinc-finger motif (22,23). Nup475 structure revealed a mainly extended region stabilized by zinc coordination and two hydrophobic cores. Secondary structure prediction of ataxin-7 block II revealed a nearly complete lack of regular secondary structural elements (data not shown). Despite the presence of a zinc coordination unit, as demonstrated by mass spectrometry (Fig. 3), absence of any stabilizing hydrophobic interactions in ataxin-7 block II suggested that it forms a novel zinc-binding fold. Furthermore, the ataxin-7 block II consensus sequence is markedly different from that of the Nup475 family, except the Cys_3His motif. Resolution of ataxin-7 block II three-dimensional structure should elucidate the folding of this atypical zinc-finger motif. Further experiments are also required to determine which residues bind zinc and whether zinc-binding is necessary for ataxin-7 incorporation into TFTC/STAGA complexes. The highly conserved residues in ataxin-7 block II between yeast SGF73 and mammalian ATX7s and the lack of high homology in their other domains suggest that these residues are involved in ataxin-7 architecture and/or interaction with other TFTC/STAGA subunits.

Block I is less conserved (16% identity between human and yeast) but is characterized by a high conservation of Cys and His forming a Cys-X_2-Cys-X_{11}-His-X_{3-4}-His/Cys motif (Fig. 2B), which is reminiscent of C_2H_2 zing-finger motifs although with a different spacing (24). Block III is found only in vertebrates ATX7, ATX7-L1 and ATX7-L2 and is characterized by the presence of several aromatic, charged and polar residues. However, it did not match any previously described motif (Fig. 2D). Function of blocks I and III remains to be elucidated, in particular whether these domains are also involved in interaction with specific TFTC/STAGA subunits. In agreement, several subunits have been shown to interact with distinct partners within these complexes (25).

Immunoprecipitation of endogenous ataxin-7 from HeLa cells specifically retrieved TFTC/STAGA subunits together with a GCN5 characteristic HAT activity. Accordingly, ataxin-7 did not interact with TBP which is specific for the TFIID transcriptional complex. Altogether, these results demonstrate that ataxin-7 is a novel subunit of TFTC-like complexes and is the orthologue of the yeast SAGA-associated factor SGF73 (Table 1). We have shown that ataxin-7 ZBD

Table 1. Subunit composition of TBP-free HAT containing complexes. Yeast and human TBP-free TAFs-HAT complexes are shown (adapted from 16,26). Subunits that are consistently found in these different complexes are presented. Yeast and human proteins within the same horizontal row show homology to each other

	TBP-free HAT complexes	
	SAGA (yeast)	TFTC/STAGA/ PCAF (human)
HAT subunit	yGcn5	hGCN5/hPCAF
TAFs	yTAF5	hTAF5/hTAF5L
	yTAF6	hTAF6/hTAF6L
	yTAF9	hTAF9
	yTAF10	hTAF10
	yTAF12	hTAF12
SPTs, ADAs	ySpt3	hSPT3
	ySpt7	hSPT7L
	Spt8	ND
	ySpt20	ND
	yAda1	hADA1
	yAda2	hADA2
	yAda3	hADA3
Other components	Tra1	TRRAP
	Sgf29	ND
	Sgf73	hATX7
	Ubp8	ND
	ND	SAP130

Sgf, SAGA-associated factor; Ubp, ubiquitin protease; SAP, spliceosome-associated protein; ND: non-defined.

(block II, residues 330–401) is sufficient to pull-down these complexes. It remains to be determined which subunit(s) directly interacts with this domain and whether ataxin-7 is required for TFTC/STAGA integrity and activity. Many TAFs paralogues can participate in TFTC formation and have redundant and complementary roles in transcriptional regulation (26). It would thus be interesting to analyze ATX7 paralogues expression profiles, whether these different proteins can be present in TFTC-like complexes and their respective roles *in vivo*. Particularly, ATX7 family members harbouring block III might have a specific function as this domain is not present in SGF73 and thus not required for SAGA complex assembly.

Ataxin-7 is the fourth member of the polyQ disease genes, besides the androgen receptor, the TBP and the atrophin-1 (36), whose normal function is involved in transcriptional regulation. Interestingly, recent findings indicate that transcriptional dysregulation contribute to the pathogenesis of polyQ-induced neuronal dysfunction (27,28) and might be mediated by defects in histone acetylation. This hypothesis is based on the observations that CREB-binding protein HAT activity is impaired by expanded polyQ *in vitro* and that histone deacetylase inhibitors are protective in Huntington's disease mouse and *Drosophila* models (29–31). Severe downregulation of genes encoding components of the phototransduction pathway has been reported consistently in photoreceptors from three different SCA7 mouse models (32–34). Thus, it is tempting to speculate that polyQ expansion in ataxin-7 would impair TFTC/STAGA HAT activity, thereby contributing to the transcriptional alterations observed in SCA7. Notably, expanded ataxin-7 aggregation might decrease the amount of TFTC/STAGA complexes containing ataxin-7 and/or sequester TFTC/STAGA subunits from their normal localization in neurons from SCA7 mouse models. However, two recent experimental evidences suggested that a partial loss of ataxin-7 function is unlikely to occur in SCA7 pathogenesis. First, Yoo *et al.* (33) recently demonstrated that SCA7 toxicity results from a gain of function mechanism using mice in which a 266 CAG repeat was targeted into the mouse *Sca7* locus. Compound heterozygous mice carrying an expanded *Sca7* allele and a *Sca7* null allele are not affected more severely than heterozygous mice carrying an expanded *Sca7* allele and a wild-type *Sca7* allele (33). Second, overexpression of normal ataxin-7 did not modulate phenotype severity in another SCA7 transgenic mouse model (34).

We demonstrated that both normal and mutant ataxin-7 can be incorporated in TFTC/STAGA complexes immunopurified from SCA7 patient cell lines and that the incorporation of mutant ataxin-7 did not alter the composition of TFTC/STAGA complexes. It will thus be of major interest to assess HAT activity from TFTC/STAGA complexes containing either normal or mutant ataxin-7. A decreased HAT activity of mutant ataxin-7 containing complexes is unlikely to occur as a partial loss of ataxin-7 function does not appear to contribute to SCA7 pathogenesis. Thus, a polyQ expansion in these complexes could lead either to an increased HAT activity or to a non-regulated transcriptional activity of the TFTC/STAGA complexes. Finally, SCA7 mice revealed selective stabilization of expanded ataxin-7 versus normal ataxin-7 (33,35). It would then be worth testing whether the reduced turnover of expanded ataxin-7 would increase the proportion of TFTC complexes containing mutant ataxin-7 and thereby contribute to SCA7 pathogenesis.

MATERIALS AND METHODS

Sequence analysis

We have used the two core domains (blocks I and II) of human ataxin-7 (ATX7) as query sequences in BLAST (37) searches in the SwissProt/TrEMBL protein sequences databases and in various genomes. We introduced the following nomenclature for human ATX7 paralogues: ATX7-L1 for KIAA1218, ATX7-L2 for FLJ00381 and ATX7-L3 for FLJ31440. Sequences were then aligned using ClustalX (38) and the figure was generated with Alscript 2.04 (39). Secondary structure of ataxin-7 block II was calculated using the PHD program (40).

Plasmids construction and GST pull-down assays

For cell transfection experiments, full-length *SCA7* cDNAs with either 10 or 60 CAGs were obtained by PCR amplification of, respectively, pαaIA and pαbIA constructs (41), using a 5′ primer encoding a FLAG epitope. These fragments were subcloned into pcDNA3.1(+) (Invitrogen) to generate pc7NFL and pc7EFL. Truncated *SCA7* constructs (pc7N456 and pc7E456) were generated by PCR amplification of pc7NFL and pc7EFL and re-introduced into pcDNA3.1(+)

vector (Invitrogen). Blocks I and II *SCA7* constructs [ATX7 (311–406), (90–406), (323–401), (330–401), (337–401), (330–389) and (330–377)] were generated by PCR amplification of pc7NFL and introduced into the pGEX-4T-1 plasmid (Amersham Pharmacia Biotech). These constructs were expressed in *Escherichia coli* BL21 (DE3) strain and purified according to manufacturer's instructions. Fusion proteins bound to glutathione–sepharose beads were incubated with NEs of HeLa cells in lysis buffer (50 mM Tris–HCl pH 7.9, 10% glycerol, 1 mM EDTA, 150 mM NaCl, 5 mM $MgCl_2$, 0.1% NP-40 and protease inhibitors). After extensive washing, bound proteins were analyzed by western blot.

Mass spectrometry measurements

Affinity purified GST–ATX7 (311–406) was recovered by elution with glutathione (GSH) and further purified by fast performance liquid chromatography on a Pharmacia Superdex S200(16/90) gel-filtration column in a buffer with 10 mM Tris–HCl pH 7.5 and 150 mM NaCl. One unit of bovine thrombin (Sigma T-6634) was added for 72 h in order to cleave the GST, which was removed finally by affinity on GSH–sepharose beads. The flow-through containing ATX7 (311–406) was then dialysed against 200 mM ammonium acetate (pH 7.0), concentrated with Centricon 3 kDa (Millipore) and submitted to electrospray ionization-time of flight mass spectrometry (LCT, Waters, UK). Samples were diluted to 10 pmol/μl in 50 mM ammonium acetate buffer and infused continuously into the ESI ion source at a flow rate of 6 μl/min through a Harvard syringe pump. Parameters were optimized so that non-covalent interactions survive the ionization/desorption process. The accelerating voltage, which controls the kinetic energy communicated to the ions in the interface region of the mass spectrometer, was set to 120 V, and the pressure to 5 mbar. The ESI-MS data were acquired in the positive ion mode in the mass range 500–4000 *m/z*. Calibration of the instrument was performed by using the multiply charged ions produced by a separate injection of horse heart myoglobine diluted to 2 pmol/μl in a 1:1 water–acetonitrile mixture (v/v) acidified with 1% of formic acid.

Western blot, IPs and HAT assays

The anti-TRRAP polyclonal (1930) and monoclonal (2TRR-2D5) antibodies were generated by immunization of rabbits and mice with peptides corresponding to aminoacids 198–219 (VKVNPEREDSETRTHSIIPRGS) and 2005–2024 (DQQPDSDMDPNSSGEGVNSV) of human TRRAP, respectively, as described (20). Western blot analyses were performed as described using anti-ataxin-7 (41), anti-TIF1β (42), anti-GCN5 (20), anti-TAF10 and anti-TBP (19) monoclonal antibodies. IPs were carried out using anti-ataxin-7 [1261, (41)] and anti-TRRAP (1930) polyclonal antibodies as described (20). Protein complexes bound to protein A–sepharose beads were either boiled and processed for western blot analysis or used for HAT assays, as described (12). TFTC complex was purified as described previously (19).

Cell transfection and immunocytofluorescence

Two × 10^5 HeLa or HEK293 cells were transfected by calcium phosphate precipitation. For immunocytofluorescence, cells were fixed in 4% paraformaldehyde and immunostaining was carried out using anti-ataxin-7 [1261 (41)] and anti-TAF10 [6TA-2B11 (19)] antibodies, as described (20).

ACKNOWLEDGEMENTS

We thank Y. Trottier and K. Merienne for discussions. We are grateful to M. Oulad-Abdelghani and G. Duval for generating the monoclonal and polyclonal TRRAP antibodies, to R. Losson for gift of anti-TIF1β antibody and to G. Stevanin for SCA7 lymphoblastoid cell lines. This study was supported by grants from Institut National de la Santé et de la Recherche Médicale, the Centre National de la Recherche Scientifique and the Hôpital Universitaire de Strasbourg (HUS) to D.D. and L.T., the Hereditary Disease Foundation and from the European Community (EUROSCA integrated project, LSHM-CT-2004-503304) to D.D. and by Association pour la Recherche sur le Cancer, the Fondation pour la Recherche Médicale, the Fonds National de la Science (FNS) ACI, European Community (HPRN-CT-2000-00087 and HPRN-CT-2000-00088), INTAS and AICR (03-084) grants to L.T. D.H. was supported by a fellowship from the Fondation pour la Recherche Médicale, S.H. by a fellowship from the Ministère de la Recherche et de la Technologie and F.R. by a fellowship from the CNRS and Région Alsace.

REFERENCES

1. David, G., Abbas, N., Stevanin, G., Durr, A., Yvert, G., Cancel, G., Weber, C., Imbert, G., Saudou, F., Antoniou, E. *et al.* (1997) Cloning of the *SCA7* gene reveals a highly unstable CAG repeat expansion. *Nat. Genet.*, **17**, 65–70.
2. Michalik, A., Martin, J.J. and Van Broeckhoeven, C. (2004) Spinocerebellar ataxia type 7 associated with pigmentary retinal dystrophy. *Eur. J. Hum. Genet.*, **12**, 2–15.
3. Kaytor, M.D., Duvick, L.A., Skinner, P.J., Koob, M.D., Ranum, L.P. and Orr, H.T. (1999) Nuclear localization of the spinocerebellar ataxia type 7 protein, ataxin-7. *Hum. Mol. Genet.*, **8**, 1657–1664.
4. Mushegian, A.R., Vishnivetskiy, S.A. and Gurevich, V.V. (2000) Conserved phosphoprotein interaction motif is functionally interchangeable between ataxin-7 and arrestins. *Biochemistry*, **39**, 6809–6813.
5. Scheel, H., Tomiuk, S. and Hofmann, K. (2003) Elucidation of ataxin-3 and ataxin-7 function by integrative bioinformatics. *Hum. Mol. Genet.*, **12**, 2845–2852.
6. Gavin, A.C., Bosche, M., Krause, R., Grandi, P., Marzioch, M., Bauer, A., Schultz, J., Rick, J.M., Michon, A.M., Cruciat, C.M. *et al.* (2002) Functional organization of the yeast proteome by systematic analysis of protein complexes. *Nature*, **415**, 141–147.
7. Sanders, S.L., Jennings, J., Canutescu, A., Link, A.J. and Weil, P.A. (2002) Proteomics of the eukaryotic transcription machinery: identification of proteins associated with components of yeast TFIID by multidimensional mass spectrometry. *Mol. Cell. Biol.*, **22**, 4723–4738.
8. Grant, P.A., Duggan, L., Cote, J., Roberts, S.M., Brownell, J.E., Candau, R., Ohba, R., Owen-Hughes, T., Allis, C.D., Winston, F. *et al.* (1997) Yeast Gcn5 functions in two multisubunit complexes to acetylate nucleosomal histones: characterization of an Ada complex and the SAGA (Spt/Ada) complex. *Genes Dev.*, **11**, 1640–1650.
9. Grant, P.A., Schieltz, D., Pray-Grant, M.G., Steger, D.J., Reese, J.C., Yates, J.R., III and Workman, J.L. (1998) A subset of TAF(II)s are integral components of the SAGA complex required for nucleosome acetylation and transcriptional stimulation. *Cell*, **94**, 45–53.

10. Yang, X.J., Ogryzko, V.V., Nishikawa, J., Howard, B.H. and Nakatani, Y. (1996) A p300/CBP-associated factor that competes with the adenoviral oncoprotein E1A. *Nature*, **382**, 319–324.
11. Xu, W., Edmondson, D.G. and Roth, S.Y. (1998) Mammalian GCN5 and P/CAF acetyltransferases have homologous amino-terminal domains important for recognition of nucleosomal substrates. *Mol. Cell. Biol.*, **18**, 5659–5669.
12. Brand, M., Yamamoto, K., Staub, A. and Tora, L. (1999) Identification of TATA-binding protein-free TAFII-containing complex subunits suggests a role in nucleosome acetylation and signal transduction. *J. Biol. Chem.*, **274**, 18285–18289.
13. Martinez, E., Kundu, T.K., Fu, J. and Roeder, R.G. (1998) A human SPT3-TAFII31-GCN5-L acetylase complex distinct from transcription factor IID. *J. Biol. Chem.*, **273**, 23781–23785.
14. Ogryzko, V.V., Kotani, T., Zhang, X., Schiltz, R.L., Howard, T., Yang, X.J., Howard, B.H., Qin, J. and Nakatani, Y. (1998) Histone-like TAFs within the PCAF histone acetylase complex. *Cell*, **94**, 35–44.
15. Grant, P.A. and Berger, S.L. (1999) Histone acetyltransferase complexes. *Semin. Cell. Dev. Biol.*, **10**, 169–177.
16. Carrozza, M.J., Utley, R.T., Workman, J.L. and Cote, J. (2003) The diverse functions of histone acetyltransferase complexes. *Trends Genet.*, **19**, 321–329.
17. Martinez, E., Palhan, V.B., Tjernberg, A., Lymar, E.S., Gamper, A.M., Kundu, T.K., Chait, B.T. and Roeder, R.G. (2001) Human STAGA complex is a chromatin-acetylating transcription coactivator that interacts with pre-mRNA splicing and DNA damage-binding factors in vivo. *Mol. Cell. Biol.*, **21**, 6782–6795.
18. Hardy, S., Brand, M., Mittler, G., Yanagisawa, J., Kato, S., Meisterernst, M. and Tora, L. (2002) TATA-binding protein-free TAF-containing complex (TFTC) and p300 are both required for efficient transcriptional activation. *J. Biol. Chem.*, **277**, 32875–32882.
19. Wieczorek, E., Brand, M., Jacq, X. and Tora, L. (1998) Function of TAF(II)-containing complex without TBP in transcription by RNA polymerase II. *Nature*, **393**, 187–191.
20. Brand, M., Moggs, J.G., Oulad-Abdelghani, M., Lejeune, F., Dilworth, F.J., Stevenin, J., Almouzni, G. and Tora, L. (2001) UV-damaged DNA-binding protein in the TFTC complex links DNA damage recognition to nucleosome acetylation. *EMBO J.*, **20**, 3187–3196.
21. Chen, S., Peng, G.H., Wang, X., Smith, A.C., Grote, S.K., Sopher, B.L. and La Spada, A.R. (2004) Interference of Crx-dependent transcription by ataxin-7 involves interaction between the glutamine regions and requires the ataxin-7 carboxy-terminal region for nuclear localization. *Hum. Mol. Genet.*, **13**, 53–67.
22. Worthington, M.T., Amann, B.T., Nathans, D. and Berg, J.M. (1996) Metal binding properties and secondary structure of the zinc-binding domain of Nup475. *Proc. Natl Acad. Sci. USA*, **93**, 13754–13759.
23. Amann, B.T., Worthington, M.T. and Berg, J.M. (2003) A Cys3His zinc-binding domain from Nup475/tristetraprolin: a novel fold with a disklike structure. *Biochemistry*, **42**, 217–221.
24. Laity, J.H., Lee, B.M. and Wright, P.E. (2001) Zinc finger proteins: new insights into structural and functional diversity. *Curr. Opin. Struct. Biol.*, **11**, 39–46.
25. Kirschner, D.B., vom Baur, E., Thibault, C., Sanders, S.L., Gangloff, Y.G., Davidson, I., Weil, P.A. and Tora, L. (2002) Distinct mutations in yeast TAF(II)25 differentially affect the composition of TFIID and SAGA complexes as well as global gene expression patterns. *Mol. Cell. Biol.*, **22**, 3178–3193.
26. Tora, L. (2002) A unified nomenclature for TATA box binding protein (TBP)-associated factors (TAFs) involved in RNA polymerase II transcription. *Genes Dev.*, **16**, 673–675.
27. Cha, J.H. (2000) Transcriptional dysregulation in Huntington's disease. *Trends Neurosci.*, **23**, 387–392.
28. Sugars, K.L. and Rubinsztein, D.C. (2003) Transcriptional abnormalities in Huntington disease. *Trends Genet.*, **19**, 233–238.
29. Steffan, J.S., Bodai, L., Pallos, J., Poelman, M., McCampbell, A., Apostol, B.L., Kazantsev, A., Schmidt, E., Zhu, Y.Z., Greenwald, M. *et al.* (2001) Histone deacetylase inhibitors arrest polyglutamine-dependent neurodegeneration in Drosophila. *Nature*, **413**, 739–743.
30. Hockly, E., Richon, V.M., Woodman, B., Smith, D.L., Zhou, X., Rosa, E., Sathasivam, K., Ghazi-Noori, S., Mahal, A., Lowden, P.A. *et al.* (2003) Suberoylanilide hydroxamic acid, a histone deacetylase inhibitor, ameliorates motor deficits in a mouse model of Huntington's disease. *Proc. Natl Acad. Sci. USA*, **100**, 2041–2046.
31. Ferrante, R.J., Kubilus, J.K., Lee, J., Ryu, H., Beesen, A., Zucker, B., Smith, K., Kowall, N.W., Ratan, R.R., Luthi-Carter, R. *et al.* (2003) Histone deacetylase inhibition by sodium butyrate chemotherapy ameliorates the neurodegenerative phenotype in Huntington's disease mice. *J. Neurosci.*, **23**, 9418–9427.
32. La Spada, A.R., Fu, Y.H., Sopher, B.L., Libby, R.T., Wang, X., Li, L.Y., Einum, D.D., Huang, J., Possin, D.E., Smith, A.C. *et al.* (2001) Polyglutamine-expanded ataxin-7 antagonizes CRX function and induces cone-rod dystrophy in a mouse model of SCA7. *Neuron*, **31**, 913–927.
33. Yoo, S.Y., Pennesi, M.E., Weeber, E.J., Xu, B., Atkinson, R., Chen, S., Armstrong, D.L., Wu, S.M., Sweatt, J.D. and Zoghbi, H.Y. (2003) SCA7 Knockin mice model human SCA7 and reveal gradual accumulation of mutant ataxin-7 in neurons and abnormalities in short-term plasticity. *Neuron*, **37**, 383–401.
34. Helmlinger, D., Abou-Sleymane, G., Yvert, G., Rousseau, S., Weber, C., Trottier, Y., Mandel, J.L. and Devys, D. (2004) Disease progression despite early loss of polyglutamine protein expression in SCA7 mouse model. *J. Neurosci.*, **24**, 1881–1887.
35. Yvert, G., Lindenberg, K.S., Devys, D., Helmlinger, D., Landwehrmeyer, G.B. and Mandel, J.L. (2001) SCA7 mouse models show selective stabilization of mutant ataxin-7 and similar cellular responses in different neuronal cell types. *Hum. Mol. Genet.*, **10**, 1679–1692.
36. Zhang, S., Xu, L., Lee, J. and Xu, T. (2002) Drosophila atrophin homolog functions as a transcriptional corepressor in multiple developmental processes. *Cell*, **108**, 45–56.
37. Altschul, S.F., Gish, W., Miller, W., Myers, E.W. and Lipman, D.J. (1990) Basic local alignment search tool. *J. Mol. Biol.*, **215**, 403–410.
38. Thompson, J.D., Gibson, T.J., Plewniak, F., Jeanmougin, F. and Higgins, D.G. (1997) The CLUSTAL_X windows interface: flexible strategies for multiple sequence alignment aided by quality analysis tools. *Nucl. Acids Res.*, **25**, 4876–4882.
39. Barton, G.J. (1993) ALSCRIPT: a tool to format multiple sequence alignments. *Protein Eng.*, **6**, 37–40.
40. Rost, B., Sander, C. and Schneider, R. (1994) PHD—an automatic mail server for protein secondary structure prediction. *Comput. Appl. Biosci.*, **10**, 53–60.
41. Yvert, G., Lindenberg, K.S., Picaud, S., Landwehrmeyer, G.B., Sahel, J.A. and Mandel, J.L. (2000) Expanded polyglutamines induce neurodegeneration and trans-neuronal alterations in cerebellum and retina of SCA7 transgenic mice. *Hum. Mol. Genet.*, **9**, 2491–2506.
42. Nielsen, A.L., Ortiz, J.A., You, J., Oulad-Abdelghani, M., Khechumian, R., Gansmuller, A., Chambon, P. and Losson, R. (1999) Interaction with members of the heterochromatin protein 1 (HP1) family and histone deacetylation are differentially involved in transcriptional silencing by members of the TIF1 family. *EMBO J.*, **18**, 6385–6395.